Two-dimensional theory of Cherenkov radiation from short laser pulses in a magnetized plasma

M. I. Bakunov,[1,2] S. B. Bodrov,[1,2] A. V. Maslov,[3] and A. M. Sergeev[2]
[1]*Department of Radiophysics, University of Nizhny Novgorod, Nizhny Novgorod 603950, Russia*
[2]*Institute of Applied Physics RAS, Nizhny Novgorod 603950, Russia*
[3]*ELORET Corporation, NASA Ames Research Center, Mail Stop 229-1, Moffett Field, California 94035, USA*
(Received 14 January 2004; published 7 July 2004)

The Cherenkov wakes excited by intense laser drivers in a perpendicularly magnetized plasma are a potential source of high-power terahertz radiation. We present a two-dimensional (2D) theory of the emission of magnetized wakes excited by a short laser pulse. The 2D model reveals the important role of the transverse size of the laser pulse missed in previous simple one-dimensional estimations of the radiation. We derived expressions for the radiated fields and for the angular/frequency distribution of the radiated energy. Beats in the radiation pattern behind the moving pulse are predicted and explained. For the interpretation of existing experimental results, the time dependence of the energy flux parallel and perpendicular to the laser path is examined.

DOI: 10.1103/PhysRevE.70.016401 PACS number(s): 52.35.Mw, 41.60.Bq, 52.59.Ye

I. INTRODUCTION

A charged particle traveling in a uniform medium with a constant speed greater than the phase velocity of light in the medium emits Cherenkov radiation [1]. The phenomenon is extensively used in experiments for counting and identifying relativistic particles [2]. First developed by Frank and Tamm [3] as early as 1937, the theory of Cherenkov radiation still attracts a lot of attention. In particular, Interesting emission features in a dispersive medium with a Lorentzian resonance were reported in recent papers [4–6].

In 1962, Askar'yan [7] predicted that in nonlinear dispersive media Cherenkov radiation can be produced by electromagnetic pulses, rather than particles. In this case, an electromagnetic pulse produces a moving pulse of nonlinear polarization which in turn can emit Cherenkov radiation. Similarly to classical Cherenkov radiation, the group velocity of the driving pulse should be greater than the phase velocity of the emitted radiation. This threshold condition can be satisfied in dispersive media when the driving pulse and emitted radiation belong to different frequency ranges. Cherenkov emission of terahertz (THz) radiation from subpicosecond optical pulses in electro-optic media has been observed experimentally [5,6,8].

Recently, a mechanism for converting large-amplitude plasma wakes (of the type used in plasma accelerators) into high-power THz radiation has been proposed [9]. In this scheme, a large-amplitude plasma wakefield is generated by an intense laser pulse (or a laser beatwave or particle bunch). By applying a magnetic field perpendicularly to the laser path, the wake becomes partially electromagnetic and develops a nonzero group velocity. This enables the wake to propagate through the plasma and to couple out into vacuum as radiation at the plasma boundary. The phenomenon may be interpreted in terms of Cherenkov radiation. Indeed, the magnetization of the plasma gives rise to the appearance of a frequency interval between the plasma (ω_p) and upper hybrid (ω_h) frequencies where the phase velocity of the extraordinary (XO) mode is less than the speed of light. Thus, the velocity threshold condition can be fulfilled for a laser pulse propagating in the plasma at nearly the speed of light, and the XO mode from the frequency interval $\omega_p < \omega < \omega_h$ can be emitted. Simple estimates made in Refs. [9–11] on the basis of the one-dimensional (1D) theory of unmagnetized laser wakefields showed that megawatt sources of THz radiation could be built with present facilities. The first experimental attempts to observe THz radiation using terawatt lasers and kilogauss magnetic fields resulted in detection of only weak radiation with several tens of milliwatts power [12,13]. Particle-in-cell simulations of the phenomenon were performed to verify the scaling laws of the radiation [10]. However, only wide (compared to the plasma wavelength c/ω_p) laser beams were considered. Meanwhile, generating large-amplitude plasma wakes requires tightly focused laser beams with focal spot radius less or even much less than c/ω_p. For example, in experiments [12,13], the laser waist was of the order of $\sim 0.1c/\omega_p$.

In this paper, we develop an analytic two-dimensional (2D) theory of Cherenkov emission from intense laser pulses in a magnetized plasma. The 2D model allows us to investigate the role of the laser beam width in the radiation process, including the most practically interesting case when the pulse width is comparable to or less than c/ω_p. Besides the practical significance, it is of general interest to study features of Cherenkov radiation produced by short laser pulses in a magnetized plasma.

The paper is organized as follows. In Sec. II, we lay out the theoretical model and basic equations. The solution of the equations using a Laplace-transform technique is given in Sec. III. We discuss the radiated fields in Sec. IV and radiated energy in Sec. V. The final Sec. VI contains concluding remarks.

II. MODEL AND BASIC EQUATIONS

We consider a short laser driver moving in a homogeneous plasma of density N at nearly the speed of light ($V_0 \approx c$) in the $+z$ direction. The transverse laser profile depends only on coordinate x and is independent of y. An external

magnetic field $\mathbf{B}_0$ is applied in the $+y$ direction. This field is uniform in space and constant in time.

To find Cherenkov radiation generated by the laser pulse, we start with Maxwell's equations

$$\frac{\partial E_z}{\partial x}+\frac{1}{V_0}\frac{\partial E_x}{\partial \xi}=\frac{1}{c}\frac{\partial B_y}{\partial \xi}, \tag{1a}$$

$$\frac{1}{V_0}\frac{\partial B_y}{\partial \xi}=\frac{1}{c}\frac{\partial E_x}{\partial \xi}-\frac{4\pi}{c}eNv_x, \tag{1b}$$

$$\frac{\partial B_y}{\partial x}=\frac{1}{c}\frac{\partial E_z}{\partial \xi}-\frac{4\pi}{c}eNv_z, \tag{1c}$$

and the equations for electron motion along the x and z axes

$$m\frac{\partial v_x}{\partial \xi}=-eE_x-e\frac{\partial \Phi}{\partial x}+\frac{e}{c}B_0v_z, \tag{2a}$$

$$m\frac{\partial v_z}{\partial \xi}=-eE_z+\frac{e}{V_0}\frac{\partial \Phi}{\partial \xi}-\frac{e}{c}B_0v_x, \tag{2b}$$

with Φ the average ponderomotive potential defined by the envelope of the laser pulse [14]. In deriving Eqs. (1) and (2), we assumed that the potential Φ and, therefore, the fields and electron velocities, depend only on x and ξ with $\xi=t-z/V_0$. This implies that pump depletion and laser instabilities are neglected.

To specify final formulas, we will use the Gaussian shape for the pulse envelope in the transverse direction:

$$\Phi(x,\xi)=\Phi_0(\xi)\exp(-x^2/\ell^2), \tag{3}$$

where ℓ is the laser spot half-width.

III. LAPLACE TRANSFORMS

To solve Eqs. (1) and (2), we will use a Laplace-transform technique. The initial conditions for the fields and electron velocities at $\xi=0$ are taken to be zero since there is no radiation ahead the laser pulse. Applying Laplace transform with respect to ξ to Eqs. (1) and (2) and eliminating the Laplace transforms of the electric field and electron velocities, we arrive at the following equation for the magnetic field transform $\widetilde{B}_y(x,s)$ (s is the Laplace variable):

$$\frac{\partial^2\widetilde{B}_y}{\partial x^2}-\kappa^2\widetilde{B}_y=F(x,s), \tag{4}$$

with function $F(x,s)$ acting as a source, given by

$$F(x,s)=-\frac{1}{c}\frac{\omega_p^2\omega_c}{s^2+\omega_h^2}\left(\frac{s^2}{c^2\beta^2}\widetilde{\Phi}+\frac{\partial^2\widetilde{\Phi}}{\partial x^2}\right), \tag{5}$$

where $\widetilde{\Phi}(x,s)=\widetilde{\Phi}_0(s)\exp(-x^2/\ell^2)$ is the Laplace transform of the ponderomotive potential

$$\kappa^2=\frac{s^2}{c^2}\left(1+\frac{\omega_p^2}{s^2}\frac{s^2+\omega_p^2}{s^2+\omega_h^2}-\frac{1}{\beta^2}\right), \tag{6}$$

where $\beta=V_0/c$, $\omega_h=\sqrt{\omega_p^2+\omega_c^2}$ is the upper hybrid frequency, $\omega_p=\sqrt{4\pi e^2N/m}$ is the plasma frequency, and $\omega_c=eB_0/mc$ is the electron cyclotron frequency.

The solution of Eq. (4) can be written as

$$\widetilde{B}_y(x,s)=-\frac{1}{2\kappa}\int_{-\infty}^{+\infty}F(x')e^{-\kappa|x-x'|}dx', \tag{7}$$

where the real part of the complex double-valued function $\kappa(s)$ should be taken positive to ensure evanescence of the fields at $x\to\pm\infty$.

The Laplace transforms of $\widetilde{E}_x$ and $\widetilde{E}_z$ are related to $\widetilde{B}_y$ by means of Eqs. (1) and (2) (in the s domain) and have the following form:

$$\widetilde{E}_x(x,s)=\frac{1}{(s^2+\omega_p^2)^2+s^2\omega_c^2}\left[\frac{s^2}{\beta}(s^2+\omega_h^2)\widetilde{B}_y-c\omega_p^2\omega_c\frac{\partial\widetilde{B}_y}{\partial x}+\frac{s^2\omega_p^2\omega_c}{\beta c}\widetilde{\Phi}-\omega_p^2(s^2+\omega_p^2)\frac{\partial\widetilde{\Phi}}{\partial x}\right], \tag{8a}$$

$$\widetilde{E}_z(x,s)=\frac{1}{(s^2+\omega_p^2)^2+s^2\omega_c^2}\left[\frac{s\omega_p^2\omega_c}{\beta}\widetilde{B}_y+cs(s^2+\omega_h^2)\frac{\partial\widetilde{B}_y}{\partial x}+\frac{\omega_p^2}{\beta c}s(s^2+\omega_p^2)\widetilde{\Phi}+s\omega_p^2\omega_c\frac{\partial\widetilde{\Phi}}{\partial x}\right]. \tag{8b}$$

Further, we will use the approximation $\beta=1$. In this approximation, Eq. (6) for $\kappa(s)$ can be simplified as

$$\kappa=\frac{\omega_p}{c}\sqrt{\frac{s^2+\omega_p^2}{s^2+\omega_h^2}}. \tag{9}$$

IV. THE RADIATED FIELDS

Expressions (7) and (8) give the solution of the problem in the s domain. To obtain the solution in the ξ domain, we have to take the inverse Laplace transform. In taking the inverse transform of $\widetilde{B}_y$ for $\xi>0$, we choose the integration contour (see Fig. 1) in the Riemann sheet in the complex s plane, where the real part of $\kappa(s)$ is positive. The branch cuts due to double-valued function $\kappa(s)$ run along the imaginary axis (where $s=i\omega$) between the branch points $\pm i\omega_p$ and $\pm i\omega_h$. At the branch cuts, function $\kappa(i\omega)$ is purely imaginary: $\kappa(i\omega)=\pm ig$, where

$$g=\frac{\omega_p}{c}\sqrt{\frac{\omega^2-\omega_p^2}{\omega_h^2-\omega^2}}, \tag{10}$$

sign "+" is taken at the right-hand side $[\mathrm{Re}(s)=0^+]$ of the upper branch cut ($\omega>0$) and left-hand side $[\mathrm{Re}(s)=0^-]$ of the lower branch cut ($\omega<0$), and sign "−" is assigned to the opposite sides of the branch cuts.

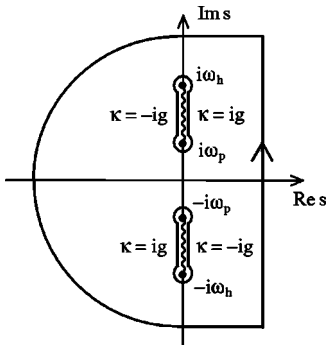

FIG. 1. Integration contour in the complex s plane.

Combining the integrals along all four sides of the branch cuts, we arrive at the following expression for the magnetic field:

$$B_y(x,\xi) = -\frac{\ell\omega_p^2\omega_c}{2\sqrt{\pi}c^3}\int_{\omega_p}^{\omega_h} d\omega \quad \left\{ \frac{e^{-(1/4)g^2\ell^2}}{g}\frac{\omega^2+c^2g^2}{\omega_h^2-\omega^2}|\widetilde{\Phi}_0| \times [\sin(\omega\xi - gx + \varphi) + \sin(\omega\xi + gx + \varphi)] \right\}, \tag{11}$$

where $\varphi(\omega)$ is the phase of $\widetilde{\Phi}_0(i\omega)$: $\widetilde{\Phi}_0(i\omega) = |\widetilde{\Phi}_0|\exp(i\varphi)$. For example, for a square pulse with duration τ, we have

$$|\widetilde{\Phi}_0| = \frac{e\tau E_L^2}{4m\omega_L^2}\frac{\sin(\omega\tau/2)}{\omega\tau/2}, \quad \varphi = -\frac{\omega\tau}{2}, \tag{12}$$

where E_L and ω_L are the laser field amplitude and frequency, respectively.

Equation (11) gives the expansion of the magnetic field $B_y(x,\xi)$ into plane waves that propagate from the laser path to $x \to \pm\infty$ (outgoing waves) and towards the laser path (incoming waves). The angle θ, at which a partial plane wave propagates with respect to the $+z$ direction, is related to the frequency of the wave by formula $\tan\theta = cg/\omega$. At large ξ, only the outgoing waves survive; the incoming waves interfere destructively. As a result, at large ξ the far-field pattern of the outgoing radiation will be formed.

The spatial distribution of the magnetic field B_y calculated on the basis of Eq. (11) is shown in Fig. 2. Three features are apparent in Fig. 2. First, the radiation pattern is conical (or wedge-shaped, in the present 2D case) that is typical for Cherenkov radiation. Second, there are beats, or multiple tails, in the field distribution. The beats disappear with increase of the transverse size of the laser pulse. Third, near the laser path, $|B_y|$ is larger for the more focused pulse. To get insight into the radiation pattern, we made an asymptotic evaluation of the integral (11) for large ξ:

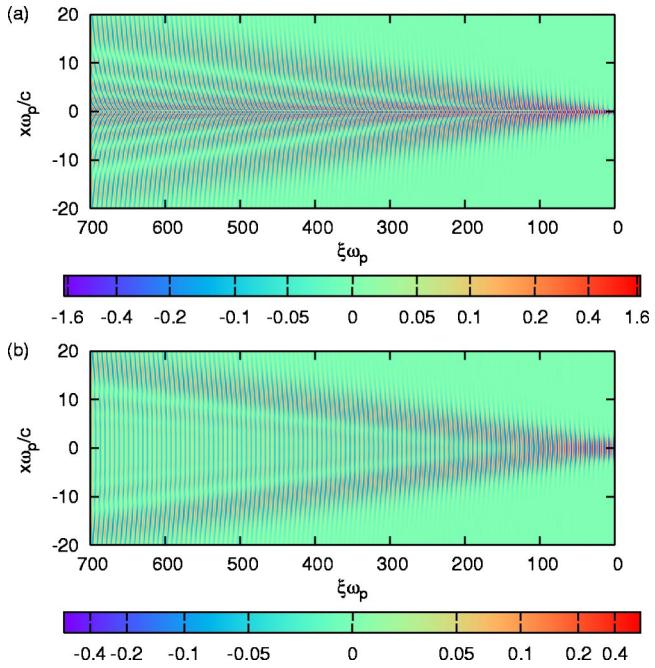

FIG. 2. (Color online). Distribution of the magnetic field B_y behind the laser driver [normalized to $|\widetilde{\Phi}_0(\omega_p)|\ell\omega_p^2\omega_c/(\sqrt{\pi}c^2)$] for (a) $\omega_p\ell/c = 0.3$ and (b) $\omega_p\ell/c = 2.0$. For both cases, $\omega_c/\omega_p = 0.3$.

$$B_y(x,\xi) \approx \frac{\ell\omega_p^2\omega_c}{2\sqrt{\pi}c^3}\sum_{i=1}^{2}\frac{e^{-(1/4)g_i^2\ell^2}}{g_i}\frac{\omega_i^2+c^2g_i^2}{\omega_h^2-\omega_i^2}|\widetilde{\Phi}_0(\omega_i)| \times \sqrt{\frac{2\pi}{|g_i''x|}}\sin\left[\omega_i\xi - g_ix + \varphi(\omega_i) - \frac{\pi}{4}\mathrm{sgn}(g_i''x)\right]. \tag{13}$$

In Eq. (13), $g_i = g(\omega_i)$, g_i'' denotes the second derivative with respect to ω taken at ω_i, and the sum is taken over the frequencies ω_i for which

$$\frac{d}{d\omega}(\omega\xi - gx + \varphi) = 0, \tag{14}$$

or

$$c\frac{dg}{d\omega} = \frac{c(\xi - \tau/2)}{x} = \cot\alpha, \tag{15}$$

where α is a half-apex angle of a cone with its apex on the moving laser pulse. Equation (15) has two roots $\omega_{1,2}$ for a fixed cone with angle $\alpha < \alpha_0$ (Fig. 3); the maximum angle α_0 corresponds in Fig. 3 to the horizontal tangent to the curve $cg'(\omega)$ ($g' = dg/d\omega$) at its minimum point. A superposition of two harmonic oscillations with frequencies ω_1 and ω_2 gives the beats in the field distribution along the cone. This explains the multitail radiation pattern visible in Fig. 2. Indeed, the beats may be interpreted as a result of the intersection of the cone with a sequence of the field tails. The beat frequency should increase with decreasing α as the two roots $\omega_{1,2}$ move farther apart (Fig. 3). This conclusion is in accord with Fig. 2. Interestingly, the radiation pattern is similar to that obtained in Ref. [5] for "subluminal" regime of Cheren-

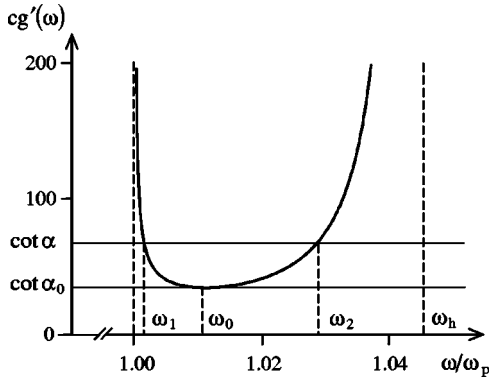

FIG. 3. Graphical solution of Eq. (15). There are two roots $\omega_{1,2}$ for $\alpha<\alpha_0$; these roots merge together at ω_0 for $\alpha=\alpha_0$. The dependence $cg'(\omega)$ is plotted for $\omega_c/\omega_p=0.3$.

kov radiation in an isotropic resonant medium.

For the cone that subtends the largest angle α_0, Eq. (15) has only one root ω_0 (Fig. 3) and, therefore, there are no beats at this overall cone (see Fig. 2). From the condition $g''(\omega)=0$, we can find the frequency ω_0 of the radiation at the overall cone ($\omega_c^2 \ll \omega_p^2$):

$$\omega_0 = \frac{\omega_p}{\sqrt{3}}\sqrt{1+2\sqrt{1+\frac{3}{4}\frac{\omega_c^2}{\omega_p^2}}} \approx \omega_p\left(1+\frac{1}{8}\frac{\omega_c^2}{\omega_p^2}\right). \quad (16)$$

Substituting ω_0 into Eq. (15) gives angle α_0:

$$\tan\,\alpha_0 \approx \frac{3\sqrt{3}}{16}\frac{\omega_c^2}{\omega_p^2}. \quad (17)$$

Substituting ω_0 into Eq. (10), we find that wave fronts at the overall cone are tilted at nearly 30° with respect to the $-z$ direction.

The disappearence of the multitail structure for the laser pulses with $\omega_p\ell/c>1$ [Fig. 2(b)] may be explained by the influence of an exponential factor in Eq. (13). For large pulse width, this factor determines significantly different amplitudes of the oscillations in sum (13) and, as a result, the beats are weakened.

To explain the effect of the field enhancement near the z axis with narrowing of the laser, it is necessary to study the spectral distribution of the radiated energy (see Sec. V).

V. THE RADIATED ENERGY

As in the classical theory of Cherenkov radiation [3], we calculate the total radiated energy per unit length of the laser path by integrating over time the energy flux per unit area far from the laser path. To find the x component of the Poynting vector S_x, we use Eq. (11) and inverse Laplace transform of Eq. (8b) for $\widetilde{E}_z$. On integrating S_x, we obtain the total radiated energy

$$W = \int_{\omega_p}^{\omega_h} w_\omega(\omega)d\omega, \quad (18)$$

where $w_\omega(\omega)$ is the spectral density of the radiation

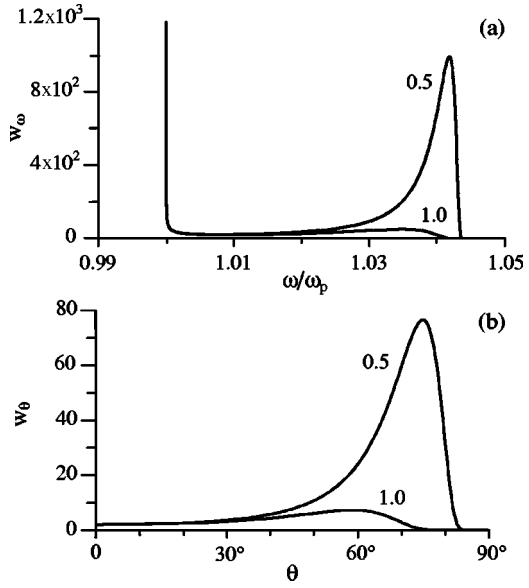

FIG. 4. (a) Spectral density of the radiated energy $w_\omega(\omega)$ [normalized to $|\widetilde{\Phi}_0(\omega_p)|^2\ell^2\omega_p^4/(16\pi c^3)$] for $\omega_c/\omega_p=0.3$ and $\omega_p\ell/c=1.0, 0.5$ (values shown near corresponding curves). (b) Corresponding angular distribution $w_\theta(\theta)$ [normalized to $|\widetilde{\Phi}_0(\omega_p)|^2\ell^2\omega_p^5/(16\pi c^3)$].

$$w_\omega(\omega) = \frac{\ell^2\omega_p^4\omega_c^2\omega}{16\pi c^4 g}\frac{\omega^2\omega_c^2-(\omega^2-\omega_p^2)^2}{(\omega_h^2-\omega^2)^3}e^{-(1/2)g^2\ell^2}|\widetilde{\Phi}_0|^2. \quad (19)$$

The spectral density of the radiated energy is shown in Fig. 4(a) for two values of the laser width. The energy flux of the laser pulse is taken the same for both curves in Fig. 4(a), i.e., $E_L^2\ell=\text{const}$, so these curves correspond to different degrees of laser focusing. The singularity at $\omega\to\omega_p$ is weak $[w_\omega(\omega)\propto(\omega-\omega_p)^{-1/2}]$ and therefore, it is integrable; its contribution into integral (18) is practically negligible. For tight focusing ($\omega_p\ell/c\ll 1$), a sharp peak in $w_\omega(\omega)$ near ω_h is formed.

The angular distribution of the radiated energy $w_\theta(\theta)$ can be found from Eq. (19) by using relation $\tan\,\theta=cg/\omega$. For a typical situation, when $\omega_c^2\ll\omega_p^2$, we obtain

$$w_\theta(\theta) \approx \frac{\ell^2\omega_p^5}{16\pi c^3}\frac{\exp\left[-\frac{1}{2}\left(\frac{\omega_p\ell}{c}\right)^2\tan^2\,\theta\right]}{\cos^4\,\theta}|\widetilde{\Phi}_0(\omega_p)|^2. \quad (20)$$

This distribution is shown in Fig. 4(b) for $\omega_p\ell/c=1.0$ and 0.5. Unlike $w_\omega(\omega)$, the function $w_\theta(\theta)$ has no peculiarity at $\theta\to 0$ (when $\omega\to\omega_p$). For $\omega_p\ell/c=0.5$, there is a peak near $\theta\approx\pi/2$. When the laser width decreases, the peak grows in magnitude and moves closer to $\pi/2$. Correspondingly, the peak in Fig. 4(a) shifts to ω_h. The plane waves with frequencies close to ω_h have a large transverse wave number $g(\omega)$, according to Eq. (10), and small group velocity ($\omega_c^2\ll\omega_p^2$)

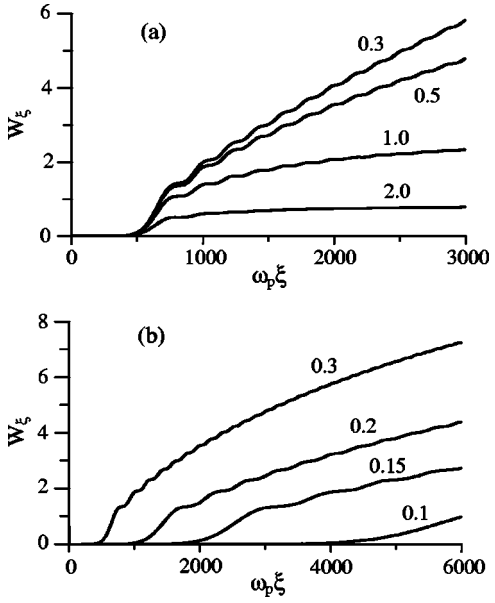

FIG. 5. The energy W_ξ [normalized to $|\widetilde{\Phi}_0(\omega_p)|^2\ell^2\omega_p^5/(16\pi c^3)$] passed to the moment ξ through the unit area placed at $x=15c/\omega_p$ as a function of ξ for: (a) $\omega_c/\omega_p=0.3$ and $\omega_p\ell/c=2.0, 1.0, 0.5, 0.3$ (values shown near corresponding curves); (b) $\omega_p\ell/c=0.5$ and $\omega_c/\omega_p=0.1, 0.15, 0.2, 0.3$ (values shown near corresponding curves).

$$v_g \approx c\frac{(\omega_h^2-\omega^2)^{3/2}}{\omega_p^2\omega_c}. \tag{21}$$

Equation (21) follows from the dispersion equation for the XO mode propagating perpendicularly to the magnetic field [15]. Thus, narrow (with $\omega_p\ell/c<1$) laser beams excite predominantly the slow waves propagating almost perpendicularly to the laser path. The slowness of the emitted waves leads to the slowness of energy spreading in the radial direction. This explains the enhancement of the field magnitude near the laser path with decreasing parameter $\omega_p\ell/c$ (see Fig. 2).

Figure 5(a), which also supports the conclusion above, shows the temporal dependence of the energy $W_\xi(\xi)=\int_0^\xi S_x(\xi)d\xi$ passed to the moment ξ through the unit area placed at $x=15c/\omega_p$ for different values of $\omega_p\ell/c$. The steps of the ladder structure visible in Fig. 5(a) [and also in Fig. 5(b) showing $W_\xi(\xi)$ for different ω_c/ω_p] correspond to the arrival of the maximums (tails) of the radiation pattern. A fine structure that oscillates at frequency of the radiated field is present in the dependence $W_\xi(\xi)$; it is not visible in Fig. 5 because of its small amplitude. Interestingly, unlike Cherenkov radiation in an isotropic medium [4], in the present case of magnetized plasma the radial energy flux as a function of ξ oscillates with change of sign (Fig. 6). The oscillations are due to the presence in XO mode of a component of the Poynting vector perpendicular to the direction of the wave propagation [16]. The waves that propagate obliquely with respect to the x axis provide the radial energy flux that oscillates and assumes both positive and negative values. The average radial energy flux is still positive.

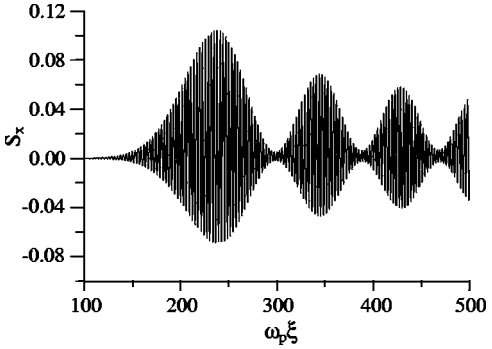

FIG. 6. The radial energy flux S_x [normalized to $|\widetilde{\Phi}_0(\omega_p)|^2\ell^2\omega_p^6/(16\pi c^3)$] at $x=15c/\omega_p$ as a function of ξ for $\omega_c/\omega_p=0.5$ and $\omega_p\ell/c=0.5$.

Although the energy $W_\xi(\xi)$ for any ξ and the total (at $\xi\to\infty$) energy W increase with decrease of the transverse size of the laser pulse [Fig. 5(a)], the rate of the energy growth at the first step of the dependence $W_\xi(\xi)$ remains practically independent of $\omega_p\ell/c$ for $\omega_p\ell/c<1$. This fact may be crucial for experimental observation of the radiation, because collisional losses can attenuate the radiation before a significant number of maximums (tails) of the radiation pattern reaches the receiver.

It may seem paradoxical that ω_c does not enter Eq. (20) and, therefore, the total radiated energy is independent of the imposed magnetic field B_0. Indeed, the possibility to produce propagating radiation is due to the presence of the magnetic field. To resolve the paradox let us note that the total radiated energy W was obtained by integration of the Poynting vector S_x over infinite time interval. The smaller ω_c the more time it takes for the fields to leave the region near the laser path [Fig. 5(b)].

In experiments [12,13], the radiation is collected by a horn antenna oriented toward the laser beam. Therefore, it is interesting to examine the energy flux of the radiation through the plane $z=$const. To find the z component of the Poynting vector S_z, we use Eq. (11) and the inverse Laplace transform of Eq. (8a) for $\widetilde{E}_x$. After integrating S_z over the infinite interval $-\infty<x<+\infty$ and averaging over the period of the field, we obtain the average power in the forward direction as

$$P_z=\int_{\omega_p}^{\omega_h} p_z(\omega)d\omega, \tag{22}$$

where

$$p_z(\omega)=\frac{\ell^2\omega_p^2\omega}{8\pi c^3 g}\frac{\omega^2\omega_c^2-(\omega^2-\omega_p^2)^2}{\omega_h^2-\omega^2}e^{-(1/2)g^2\ell^2}|\widetilde{\Phi}_0|^2. \tag{23}$$

For $\omega_c^2\ll\omega_p^2$, the approximation $\omega^2\omega_c^2-(\omega^2-\omega_p^2)^2\approx\omega_p^2\omega_c^2$ can be used in Eq. (23) so that Eq. (22) may be reduced to a form convenient for estimations, as

$$P_z \approx \frac{\ell^2 \omega_p^3 \omega_c^2}{16\pi c^2} |\widetilde{\Phi}_0(\omega_p)|^2 I, \tag{24}$$

with dimensionless factor

$$I = \int_1^{x_h} \frac{dx}{\sqrt{x_h - x}\sqrt{x-1}} \exp\left[-\frac{1}{2}\left(\frac{\omega_p \ell}{c}\right)^2 \frac{x-1}{x_h - x}\right], \tag{25}$$

where $x_h = \omega_h^2/\omega_p^2 = 1 + \omega_c^2/\omega_p^2$. A numerical investigation of integral (25) shows that the factor I varies very little in a wide range of the parameters $\omega_p \ell/c$ and ω_c/ω_p: $I \approx 2$ to 4 for $0.1 \leqslant \omega_p \ell/c \leqslant 3$ and $0.01 \leqslant \omega_c/\omega_p \leqslant 0.3$. Therefore, two essential conclusions can be made from Eq. (24). First, the radiating power is practically independent of laser focusing in the interesting range of the parameter $\omega_p \ell/c$. Indeed, it follows from Eq. (12) that $|\widetilde{\Phi}_0(\omega_p)| \propto E_L^2$ and thus, the variables ℓ and E_L enter Eq. (24) only in combination $E_L^2 \ell$, which is constant for laser pulses with the same energy. Second, the radiating power depends rather strongly on the plasma frequency: $P_z \propto \omega_p^3$.

Now let us esimate the radiating power P_z given by Eq. (24) for the conditions of the experiments [12,13]. Taking laser intensity 10^{17} W/cm^2, wavelength 800 nm, $\tau = 100$ fs, $\ell = 10$ μm, $\omega_p/2\pi = 2$ THz, and $\omega_c/\omega_p = 0.01$, we obtain from Eq. (24)

$$P_z \approx 350 \text{ W}. \tag{26}$$

The radiating power detected in experiments [12,13] was estimated to be only about several tens of milliwatts. There seems to be a large discrepancy between the experimental result and estimation (26). To explain the discrepancy, let us note that the detected frequency of the radiation was ten times lower than the expected one; i.e., $\omega_p/10$ rather than ω_p [12]. The latter fact indicates that the detected radiation arrived not from the plasma volume, but from the smooth transition layer that existed between the plasma and vacuum. In this layer, the plasma density drops from ω_p to 0. By substituting the experimentally measured frequency $\omega_p/10$ instead of ω_p into Eq. (24), we obtain

$$P_z \approx 500 \text{ mW}, \tag{27}$$

which fits much better the experimental data. This agreement shows that Eq. (24) can be used for quantitative estimates of the power yield from Cherenkov wakes.

VI. CONCLUSION

To conclude, we have developed a 2D theory of the emission of magnetized wakes excited by a short laser pulse. This theory is directly related to the experimental situation when cylindrical lenses are used to focus the laser beams and the beam is extended in one transverse direction and tightly focused in the other direction. For three-dimensional focusing, the 2D model can give a qualitative physical insight into the role of the transverse size of the laser pulse in the wake emission that was completely missed in previous simple 1D estimations of the Cherenkov wakes [9–11].

In particular, we have shown that Cherenkov radiation excited by a focused laser pulse with transverse size ℓ such that $\omega_p \ell/c \leqslant 1$ forms a multitail conical structure with the apex at the moving laser pulse. The energy radiated in the radial direction has a steplike dependence on time that corresponds to the arrival of the radiation tails at the unit area far from the laser path. The total radiated energy increases with decreasing the parameter $\omega_p \ell/c$. However, this raise in the radiated energy is attributed mainly to the harmonics that have frequencies $\omega \approx \omega_h$ and low group velocities. Collisional losses can attenuate these spectral parts of the radiation before they reach the receiver. Therefore, the effect of the growth of the radiated energy for a more tight laser focusing may not be easily registered in experiment.

For the interpretation of existing experimental results, we derived a simple formula [Eq. (24)] for the average power P in the forward (along the laser path) direction. According to the estimations of Refs. [9,10], made on the basis of 1D approximation, this power should be independent of the plasma density. On the contrary, our formula (24) predicts strong dependence of P on the plasma density: $P \propto \omega_p^3$. In fact, this prediction is indirectly supported by the experimental results of Ref. [12].

In addition, in 1D approximation, the energy-flux density of the radiation in forward direction is proportional to E_L^4 [9,10]. Applying this approximation to 2D laser focusing by cylindrical lenses gives for the power $P \propto E_L^4 \ell$ or $P \propto (E_L^4 \ell^2)/\ell$; i.e., the power grows infinitely as $\ell \to 0$. Our rigorous calculations show [Eq. (24)] that, in fact, the radiating power P depends rather weakly on the laser pulse width in the practically interesting interval $0.1 \leqslant \omega_p \ell/c \leqslant 3$.

This work was supported in part (M. I. B., S. B. B., and A. M. S.) by the program "Femtosecond optics and physics of super-strong laser fields" of the Presidium of RAS.

[1] P. A. Cherenkov, Dokl. Akad. Nauk SSSR **2**, 451 (1934); S. Vavilov, *ibid.* **2**, 457 (1934).
[2] J. Seguinot and T. Ypsilantis, Nucl. Instrum. Methods Phys. Res. A **433**, 1 (1999), and references therein.
[3] I. Frank and I. Tamm, Dokl. Akad. Nauk SSSR **14**, 109 (1937).
[4] G. N. Afanasiev, V. G. Kartavenko, and E. N. Magar, Physica B **269**, 95 (1999).
[5] T. E. Stevens, J. K. Wahlstrand, J. Kuhl, and R. Merlin, Science **291**, 627 (2001).
[6] J. K. Wahlstrand and R. Merlin, Phys. Rev. B **68**, 054301 (2003).
[7] G. A. Askar'yan, Zh. Eksp. Teor. Fiz. **42**, 1360 (1962) [Sov. Phys. JETP **15**, 943 (1962)]; Phys. Rev. Lett. **57**, 2470 (1986).
[8] D. H. Auston, K. P. Cheung, J. A. Valdmanis, and D. A. Kleinman, Phys. Rev. Lett. **53**, 1555 (1984).
[9] J. Yoshii, C. H. Lai, T. Katsouleas, C. Joshi, and W. B. Mori, Phys. Rev. Lett. **79**, 4194 (1997).

[10] N. Spence, T. Katsouleas, P. Muggli, W. B. Mori, and R. Hemker, Phys. Plasmas **8**, 4995 (2001).

[11] C. Guang *et al.*, *Conference Digest of the 27th International Conference on Infrared and Millimeter Waves, San Diego, 2002* (IEEE, San Diego, CA, 2002), pp. 17–18.

[12] N. Yugami, T. Higashiguchi, H. Gao, S. Sakai, K. Takahashi, H. Ito, Y. Nishida, and T. Katsouleas, Phys. Rev. Lett. **89**, 065003 (2002).

[13] D. Dorranian, M. Starodubtsev, H. Kawakami, H. Ito, N. Yugami, and Y. Nishida, Phys. Rev. E **68**, 026409 (2003).

[14] W. L. Kruer, *The Physics of Laser Plasma Interactions* (Addison-Wesley, New York, 1988).

[15] F. F. Chen, *Introduction to Plasma Physics and Controlled Fusion I*, 2nd ed. (Plenum, New York, 1984).

[16] V. L. Ginzburg, *Propagation of Electromagnetic Waves in Plasma*, 2nd ed. (Pergamon, 1970).